Supplementary material for "Bianisotropy and magnetism in plasmonic gratings"

Matthias Kraft, Avi Braun, Yu Luo, S. A. Maier and J.B. Pendry

April 27, 2016

S1 Profile of the simulated connected and control grating

Here we give the cross-sections of the connected and control grating that have been used in the COMSOL simulations. The dimensions were chosen to best match those extracted from SEM images of the experimental structure. We rounded the corners to avoid unphysical singularities. The rounding was done using the 'Fillet'-tool in COMSOL 4.3a with rounding radius 21.8nm for the connected and 13.75nm for the control grating. The surrounding medium had a refractive index of $N = 1.46$, whereas permittivity data for evaporated gold [1] was used for the gratings.

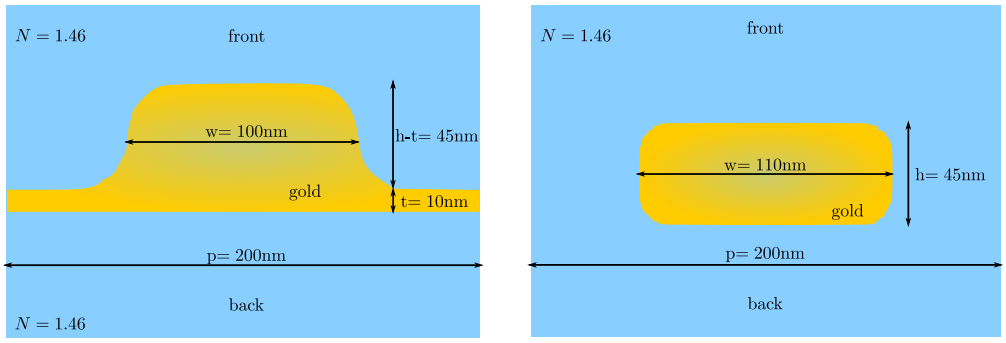

Figure S1: Grating profiles as used in the COMSOL simulations.

S2 Mode profile and energy density at the plasmon resonance

Figure S2 shows the reflection spectrum of the connected grating for front illumination with $P = 90$, as is plotted in figure 3 of the main manuscript. Here, we additionally show the electric field and energy density distributions at the plasmon resonance. We note that the resonance is split into a mode existing mostly in between the grating lines (low frequency) and a mode concentrated on/in the grating lines (high frequency), thus indicating the presence of a band gap [2]. The same mode profiles can be observed for reflection from the back. However, in this case the reflection peak is much stronger and the tails overlap such that there is no reflection dip between the modes. The experimental data in figure 3 of the main paper also does not show the dip in reflection, we attribute this to fabrication imperfections, e.g. non-uniform pitch leading to slight shifts in the resonance positions, thus 'washing' the reflection dip out.

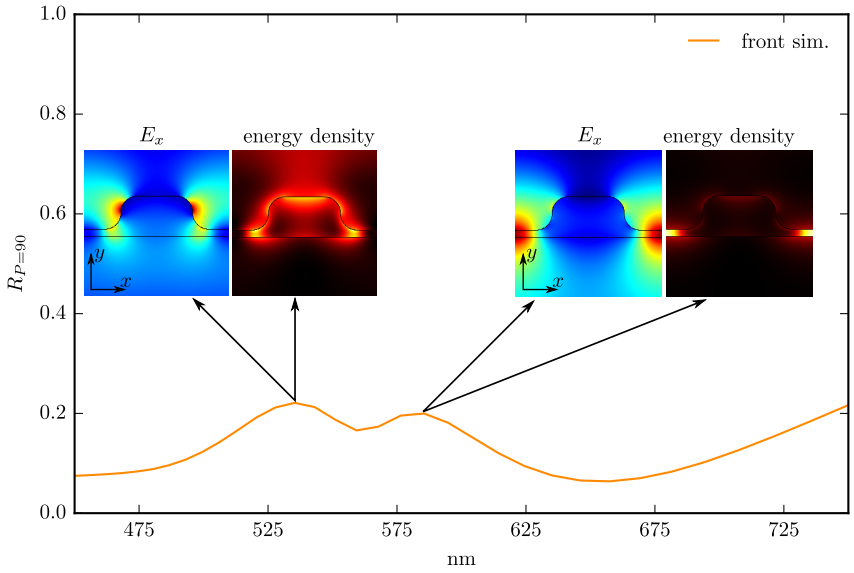

Figure S2: Simulated reflection spectrum for front illumination and P= 90. The insets show the horizontal (as drawn) component of the electric field and the energy density at the plasmon resonance.

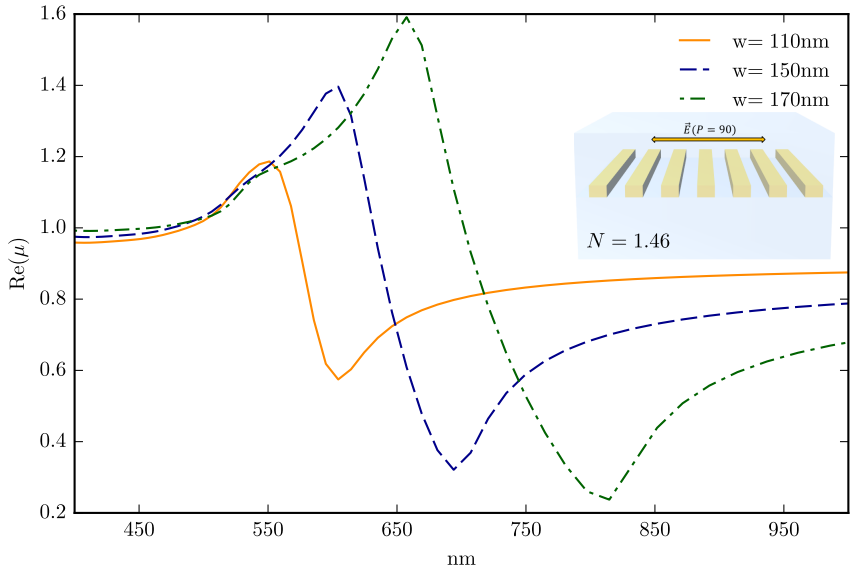

Figure S3: Effective permeability retrieved from simulations versus wavelength. Unconnected gratings with different widths of the grating lines are compared. The solid orange line with w= 110nm correpsonds to the control grating presented in the main paper. The incident light was polarized perpendicular to the grating lines.

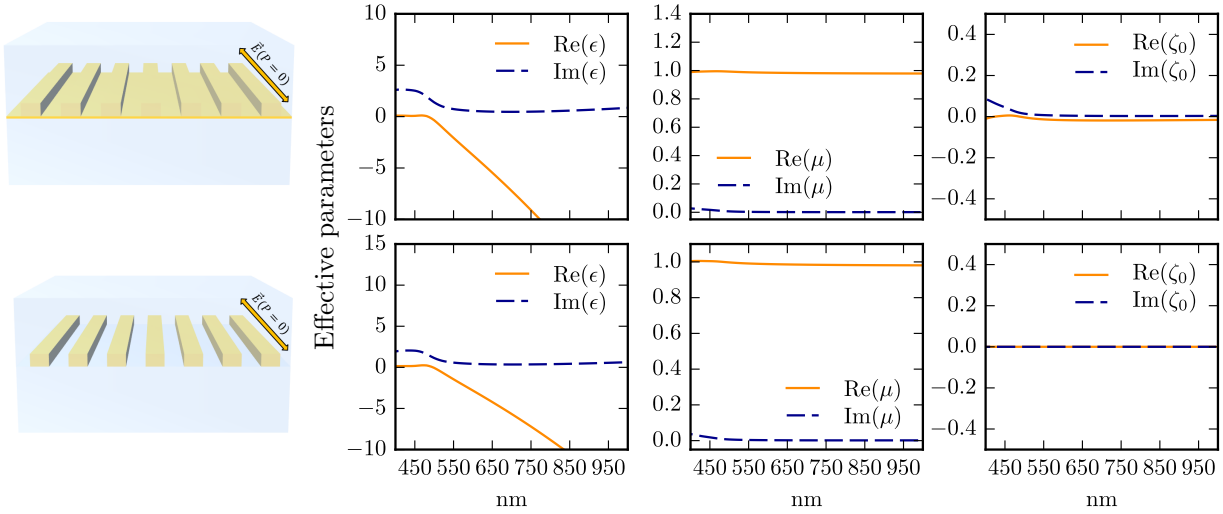

Figure S4: Effective material parameters retrieved from numerical simulations of the gold gratings described in figure 1 of the main manuscript. Results are for $P = 0$. The left column shows the effective permittivity, the middle column shows the effective permeability and the right column shows the bianisotropic coupling parameter. We used standard retrieval methods [4, 5, 6] and assumed a symmetric metamaterial slab with thickness d_{eff} equal to the maximum thickness of the gold gratings, i.e. $d_{eff} = 55$nm for the connected (top) and $d_{eff} = 45nm$ for the unconnected grating (bottom).

S3 Diamagnetic effect in the control grating

Figure S3 shows the effective permeability retrieved from COMSOL simulations of the unconnected grating under $P = 90$ incidence. We compare the effective permeability for different widths of the grating lines. Since we keep the period fixed, this means the gap between neighboring grating lines is reduced. Note that the permeability does not converge to unity in the long wavelength limit, but to a value below, indicating a diamagnetic response [3]. The wider the grating lines, i.e. the smaller the gap between them, the stronger this effect. This is in line with the explanations given in section 2.2 of the main paper.

S4 Effective material parameters for P=0

In figure S4 we look at the effective material parameters for $P = 0$. Here, the electric field is polarized along the grating lines and current can flow freely in both the control and bi-anisotropic gratings, similar to the current flow in thin gold films. The lack of a plasmon resonance leads to a near-zero magneto-electric coupling for the connected gold grating.

S5 Enlarged SEM images

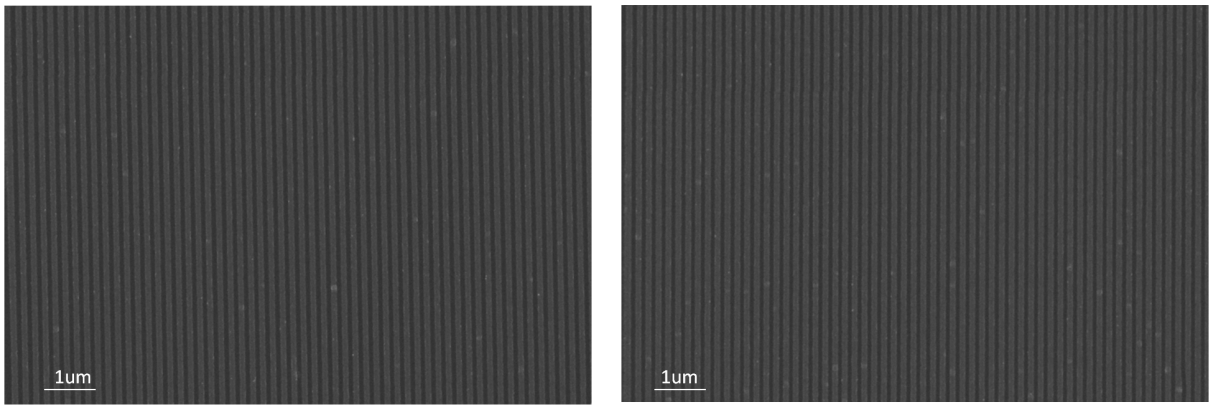

Figure S5: SEM image of the connected gold grating (left) and the unconnected control grating (right). Both gratings show a good uniformity throughout.

References

[1] Robert L. Olmon, Brian Slovick, Timothy W. Johnson, David Shelton, Sang-Hyun Oh, Glenn D. Boreman, and Markus B. Raschke. Optical dielectric function of gold. *Phys. Rev. B*, 86:235147, Dec 2012.

[2] W. L. Barnes, T. W. Preist, S. C. Kitson, and J. R. Sambles. Physical origin of photonic energy gaps in the propagation of surface plasmons on gratings. *Phys. Rev. B*, 54:6227–6244, Sep 1996.

[3] B Wood and J. B. Pendry. Metamaterials at zero frequency. *Journal of Physics: Condensed Matter*, 19(076208), 2007.

[4] Xudong Chen, Bae-ian Wu, Jin Au Kong, and Tomasz M Grzegorczyk. Retrieval of the effective constitutive parameters of bianisotropic metamaterials. *Phys. Rev. E*, 71(046610):1–9, 2005.

[5] Zhaofeng Li, Koray Aydin, and Ekmel Ozbay. Determination of the effective constitutive parameters of bianisotropic metamaterials from reflection and transmission coefficients. *Phys. Rev. E*, 79:026610, Feb 2009.

[6] Christine E Kriegeler, Michael Stefan Rill, Stefan Linden, Martin Wegener, and A Split-ring Resonators. Bianisotropic Photonic Metamaterials. *IEEE J. Quant. Electron.*, 16(2):367–375, 2010.